Proc. Natl. Acad. Sci. USA
Vol. 92, pp. 11303–11306, November 1995
Neurobiology

Spatial heterogeneity of inhibitory surrounds in the middle temporal visual area

(receptive fields/cortex/macaque)

D.-K. XIAO*, S. RAIGUEL*, V. MARCAR*, J. KOENDERINK†, AND G. A. ORBAN*‡

*Laboratorium voor Neuro- en Psychofysiologie, Katholieke Universiteit Leuven, School of Medicine, Campus Gasthuisberg, B-3000 Leuven, Belgium; and †Utrecht Biophysics Research Institute, University of Utrecht, P.O. Box 80000, 3508 TA Utrecht, The Netherlands

Communicated by James M. Sprague, University of Pennsylvania Medical Center, Philadelphia, PA, August 14, 1995 (received for review April 14, 1995)

ABSTRACT **A recurrent theme in the organization of vertebrate visual cortex is that of receptive fields with an associated "silent" opponency component. In the middle temporal area (area MT), a cortical visual area involved in the analysis of retinal motion in primates, this opponency appears in the form of a region outside the classical receptive field (CRF) that in itself gives no response but suppresses responses to motion evoked within the CRF. This antagonistic motion surround has been described as very large and symmetrically arrayed around the CRF. On the basis of this view, the primary function of the surround has long been thought to consist of simple figure-ground segregation based on movement. We have made use of small stimulus patches to map the form and extent of the surround and find evidence that the surround inhibition of many MT cells is in fact confined to restricted regions on one side or on opposite sides of the CRF. Such regions endow MT cells with the ability to make local-to-local motion comparisons, capable of extracting more complex features from the visual environment, and as such, may be better viewed as intrinsic parts of the receptive field, rather than as separate entities responsible for local-to-global comparisons.**

The antagonistic surround mechanism is a recurring principle throughout the visual systems of vertebrates (1–3). It has been extensively studied in primate intermediate visual cortical areas, where the surround is more complex in function than at earlier levels of the visual system. Surround mechanisms are well documented in cortical visual area V4, for example (4–8), where they are thought to underlie color constancy. Antagonistic surrounds have been most extensively investigated in the middle temporal visual area (area MT) (9–12), an area intimately associated with retinal motion processing (13–18). These silent surrounds are generally assumed to completely encircle (18) the classical receptive field (CRF), where they produce no response on their own, but reveal their presence only through the suppression of the responses arising from the CRF when stimuli extend beyond the CRF (19, 20). The functional relevance of surrounds is underscored by the vertical (laminar) and horizontal (columnar) organization of surround influence within area MT (10–12).

Most functions commonly attributed to the antagonistic surround in area MT, such as figure–ground segregation, differentiation of object motion from self motion, and instigation of attention (18, 21, 22), have assumed that the surround completely envelopes the CRF and acts as a local-to-global comparison mechanism. Theoretical considerations (23–26) have suggested that a nonsymmetric surround could be of much greater computational utility, particularly with regard to computing three-dimensional structure from motion, which is impaired by MT lesions (27). Previously, authors have speculated (23) on the existence of such surrounds but have conceded that evidence for such surrounds was lacking. Given the theoretical importance of asymmetry in the region outside the CRF, we have investigated the surround by using small stimuli to resolve its spatial configuration in finer detail.

METHODS

The spatial distribution of surround inhibition in area MT was studied by extracellular recording techniques (19) in 12 anesthetized and paralyzed monkeys (*Macaca fascicularis*), weighing between 3.2 kg and 5.4 kg. All cells studied showed a response inhibition of at least 50% for a full-screen stimulus compared to stimulation of the CRF area alone. The basic stimulus consisted of white random dots on a dark background, moving coherently in the frontoparallel plane (13–17) at the optimum speed and direction of motion. These parameters, as well as stimulus position and size, were optimized for each neuron during the preliminary testing as described in ref. 20. Stimuli were viewed at 57 or 28 cm, depending on the receptive field (RF) size. At 57 cm, the dots measured 0.35° in diameter with a density of 2.5 dots per square degree, and the display measured 25.6° × 25.6°. Data were collected from 10 or more presentations of all stimulus conditions. Tests examining the spatial structure of the surround utilized a stimulus covering the CRF plus one or two "probe" stimuli positioned in the surround. The first of these tests, the surround asymmetry test (SAT), used a circular probe stimulus (Fig. 1*A*) to test eight positions arranged symmetrically around the CRF. These positions were tested either singly (position test), to quantify the levels of inhibition in each of the eight positions around the CRF individually or two at a time (axis test) by using pairs of positions on opposite sides of the CRF, to measure inhibition along four different axes (Fig. 1*B*). The surround mapping test (SMT) utilized a probe stimulus presented in 24 of the 25 positions in a 5 × 5 grid (Fig. 1*C*), with the center most position containing the CRF stimulus. This mapped the surround influence as a two-dimensional contour plot. For further analysis, inhibition elicited at a given position was expressed as the percent change from the control (CRF alone) stimulus.

A selectivity index (SI) quantifying the degree of surround symmetry was computed for each cell tested with the SAT by using the formula

The publication costs of this article were defrayed in part by page charge payment. This article must therefore be hereby marked "*advertisement*" in accordance with 18 U.S.C. §1734 solely to indicate this fact.

Abbreviations: area MT, middle temporal area; RF, receptive field; CRF, classical RF; SAT, surround asymmetry test; SMT, surround map test; SI, selectivity index.

‡To whom reprint requests should be addressed.

$$SI = \frac{\sqrt{\left\{\sum_{j=1}^{n} Sj \cdot \sin[2\pi \cdot (j-1)/n]\right\}^2 + \left\{\sum_{j=1}^{n} Sj \cdot \cos[2\pi \cdot (j-1)/n]\right\}^2}}{\sum_{j=1}^{n} Sj},$$

where n is the number of positions tested (eight for the position test and four for the axis test) and S is the inhibition elicited by the probe stimulus in a given position (28). This angularly weighted SI gives a value between 1 for a completely asymmetrical response (only one position shows inhibition) and 0 for a completely circularly symmetric response (all positions show equal inhibition). Two SI values, the SI_{p1} and SI_{p2}, were calculated from each position test. The first, the SI_{p1}, is based upon the inhibition elicited by each of the eight positions of the position test taken one at a time. This index is maximal when the inhibitory influence is confined to a single position and appears as a single peak on one side of the CRF in the SMT. The SI_{p2} is calculated from the same data but analyzed pairwise, taking the total inhibition elicited by the four pairs of positions situated opposite one another. This SI will be largest when the inhibition is concentrated along a single axis and appears as two peaks flanking the CRF. Thus, the relative sizes of these two SIs give an indication of the degree of symmetry associated with the surround modulation. A third index, the SI_a, was calculated by using the data from the axis test. This test utilized the same four pairs of positions as those used in deriving SI_{p2} but the data were obtained by stimulating both positions simultaneously. Differences between the SI_a and the SI_{p2} are indicative of higher-order surround interactions. An SI value of 0.15, which corresponds to a ratio of approximately 2:1 in the inhibition strength at any two positions or axes, was chosen as the criterion level above which surround influence was considered heterogeneous.

RESULTS

In all, 102 MT cells were recorded. Of these cells, 86 were tested with the SAT, 32 of which were also tested with the SMT (Fig. 1). The remaining 16 cells were tested only with a preliminary version of the SAT employing 16 pie-shaped segments (18) that gave qualitative evidence of distinct surround inhomogeneity in 6 of those cells. The prevalence of surround heterogeneity was obvious even by direct comparison of the responses in the SAT: In 33 cells (38%), a single surround position inhibited the response by more than 50% while one or more of the remaining positions elicited no inhibition. In a number of cells, one or more of those positions even showed a facilitation that exceeded 50% in 19 cells and was statistically significant in seven cases ($P < 0.05$, Wilcoxon paired sample test). The distribution of the ratios between highest and lowest response, for each of the eight surround positions in each cell, provides further indication of the predominence of heterogenous surrounds. In 72 cells (84%), this ratio was greater than 2. Position had a statistically significant effect in 39 of the cells test ($P < 0.05$, one-way ANOVA).

The SAT reveals that surround strength varies systematically with the angular position of the probe stimulus in the surround and that this variation can be characterized according to one of three patterns, listed here in order of decreasing surround symmetry: (*i*) those in which the surround strength is independent of position (circularly symmetric); (*ii*) those in which the inhibition is concentrated in two patches mirrored on either side of the CRF (bilaterally symmetric), and (*iii*) those in which inhibitory activity is concentrated in a single region on one side of the CRF (asymmetric). Classification of cells into the above three categories is based on the relative magnitudes of the SI_{p2} and SI_{p1}: If neither exceeds 0.15, the cell is considered circularly symmetric (23%). If either exceeds 0.15, then the cell is classified according to which of the two is greater. If the SI_{p2} is larger, then the cell is considered bilaterally symmetric (32%), if the SI_{p1} is larger, then the cell is considered asymmetric (45%). An example of each of these three classifications is shown in Figs. 2 and 3. The SIs were distributed as follows in the sample: median $SI_{p1} = 0.16$; quartiles = 0.09 and 0.30; median $SI_{p2} = 0.15$; quartiles = 0.07 and 0.24; for the axis test, median $SI_a = 0.16$; quartiles = 0.09 and 0.28.

The surround maps, like those in Figs. 2*D* and 3 *A* and *D*, verify the type of symmetry shown by the SAT and visualize the distribution of the surround in a more intuitive, albeit qualitative, manner. Fig. 2 also illustrates another general observation about bilaterally symmetric surround inhibition—that the axis of the inhibition tended to be orthogonal (median 90°) to the long axis of elliptical CRFs. The distribution of this angle differed significantly from uniform distribution ($\chi^2 = 14.25$; $P < 0.001$). The axis or position of the inhibitory regions also showed a tendency to lie close to the preferred direction of motion ($\chi^2 = 10.41$; $P < 0.005$), in accordance with a previous report (12) that the long axis of the RF tends to be oriented orthogonal to the preferred direction. However, all possible

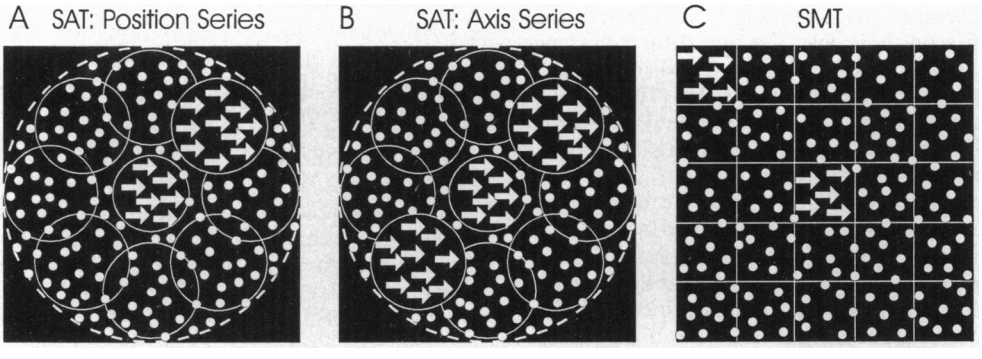

FIG. 1. Diagram of the stimuli used in the surround tests. (*A* and *B*) Position and axis series of SAT. Arrows indicate moving dots. Lines delineating borders of stimuli were not present in the actual stimuli. The SAT consisted of nine circular areas, one central area covering the CRF and eight others positioned around the CRF at 45° intervals. The circles in the surround extended from within 1° of the CRF to the edge of the display. The center area was stimulated alone (CRF control), with one of the areas in the surround (position series) (*A*), or with two of the areas in the surround placed 180° apart (axis series) (*B*). A full screen stimulus was also added as a control. (*C*) SMT. In this test the screen was divided into 25 equal squares 5° on a side at a distance of 57 cm. A stimulus square was presented in the central position alone (as the control) or in combination with a probe square in one of the remaining 24 positions.

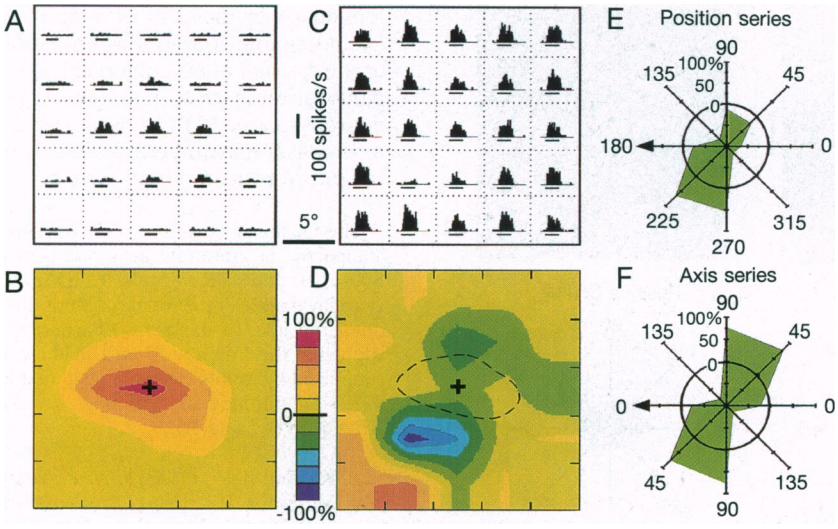

FIG. 2. Layer 3c MT cell, at eccentricity 18.2°, that had a bilaterally symmetric surround. (*A* and *B*) CRF mapping test. (*C* and *D*) SMT. (*E* and *F*) SAT. (*A*) The peristimulus time histograms (PSTHs) of the CRF mapping test (10 trials). Horizontal bars under histograms indicate the stimulus presentation period (320 ms). The 5° calibration bar applies to both *A* and *C*. (*B*) CRF mapped the normalized responses to a single stimulus patch in 25 positions, plotted as a function of stimulus position, on a five-level isoresponsive contour plot, with interpolated values between positions (20). The crosses in this and other maps indicate the center of mass of the CRF. The calibration bar applies to both *B* and *D*. Positive values represent excitation or facilitation; negative values indicate inhibition. (*C*) The PSTHs for the SMT (13 trials). Histograms in each square show responses when two areas were stimulated simultaneously, one in the center covering the CRF and another in the position shown by the square. The center-most square shows the response to the center stimulus alone. (*D*) Data from *C* presented as a 10-level isomodulation contour plot, showing inhibition or facilitation of center response by stimuli in the other 24 squares. Values between positions are interpolated. The dashed oval indicates the 50% response level shown in *B*. This cell illustrates the principle that the long axis of a elliptical cell, which in this example is near the horizontal, tends to be orthogonal to the axis of the inhibition, which is near vertical in this SMT. (*E*) The strength of the inhibition elicited by each stimulus of the SAT position series plotted in polar coordinates. The angle reflects the eight positions of the probe stimulus in the surround and is expressed relative to the preferred direction of motion (arrow). Circle shows the response level with center stimulus alone (no inhibition) and the distance from the origin represents the degree of inhibition. Negative values (inside the circle) represent facilitation. With an SI_{p2} value of 0.41 and an SI_{p1} value of 0.25, this cell was classified as an bilaterally symmetric surround cell. (*F*) Inhibition in the axis series of the SAT plotted in polar coordinates (same conventions as in *E* except each of four positions was plotted symmetrically). The cell retained its bilaterally symmetric surround. In this test, $SI_a = 0.45$. The response to the center circle alone was 49 spikes per s, and the full screen evoked an inhibition of 90%.

angles between the RF and the preferred direction occurred within the sample population.

Comparison of the SI_{p2} and SI_a tests in which one or two probe stimuli were present in the surround revealed a further degree of complexity in the spatial structure of the inhibitory regions outside the CRF. About half of the cells that had been shown to be either asymmetric or bilaterally symmetric in the position series appeared circularly symmetric when tested in the axis series of SAT (Figs. 2 and 3). This suggests that inhibitory regions outside the CRF in some cells have subliminal tails (29), which may explain why earlier investigators (9, 18) have reported more uniform surrounds.

DISCUSSION

It is clear that the classical concept of a uniform antagonistic surround applies only to a minority of MT cells. The CRF of many MT cells is in fact flanked by discrete inhibitory regions that are capable of engaging in more complex operations performed upon the motion signal and, as such, should be considered an integral part of the RF, albeit a composite RF. It is important to distinguish between an aspecific surround and more specialized inhibitory regions. The former is not intrinsic to the operations performed by the CRF but simply acts as a spatial filter for rejecting uniform motion, whereas the latter contributes to higher-level operations performed by the neuron. In the first case, the surround can be masked without altering the basic functional role of the neuron but not in the second case.

Although we speak of asymmetrical surround influences as arising exclusively from inhomogeneities in the surround, it might be argued that they could also arise from an asymmetric CRF. Some ambiguity in this regard is unavoidable because the surround itself cannot be tested in isolation, but only mapped in terms of its effect upon the CRF response. The surround in Fig. 2*D*, for example, might appear bilobal as a result of overlap with the elongated CRF that cancels or overrides the inhibition on the right and left, and a certain amount of overlap has in fact been shown between the excitatory and inhibitory RF components in area MT (12). Nonetheless, there are several indications that the conformation of the surround itself is responsible for the observed inhomogeneites. The center stimulus in the SAT tests, which is adjusted to the optimum diameter of the CRF, drives the CRF at maximum or near-maximum capacity. Any response evoked by a second probe stimulus will, thus, sum poorly with that evoked from the CRF, evoking little if any additional spike activity that could compete with the surround influence at a given point. Furthermore, manifestations of surround heterogeneity were often too distally located to be associated with the CRF. In both Figs. 2*D* and 3*A*, there are peaks of facilitation and inhibition located some distance from the CRF. Finally, if asymmetric or elliptical CRFs produce uneven surround influences, then a relationship should exist between the shape of the CRF and the degree of symmetry shown by the surround. For example, highly elliptical CRFs, like that in Fig. 2, should show a higher tendency to produce bilaterally symmetric surround influences. Plotting the SI_{p2} as a function of the percent difference between the long and short axes, however, failed to show such a relationship (slope $= 1.1 \times 10^{-3}$; intercept $= 0.14$; $R^2 = 2.5 \times 10^{-2}$). In the final analysis, however, it is probably irrelevent from a functional standpoint which of these two mechanisms leads to the observed asymmetry, since the output of the cell will be identical in either case.

Mathematically (25), optic flow processing can be implemented in several equivalent ways. Present findings indicate an

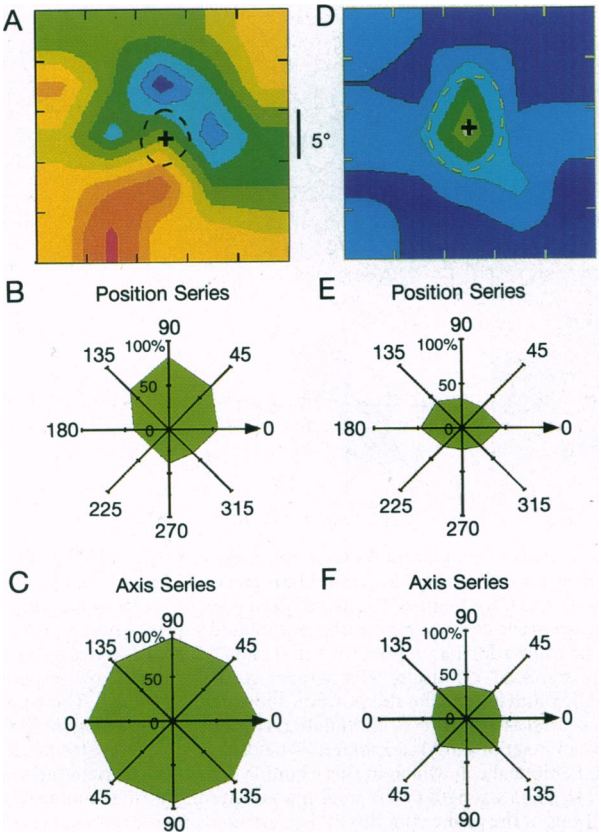

FIG. 3. (*A–C*) Asymmetric cell (cell 6824, a layer-5 cell at 1.3° eccentricity). (*D–F*) Circularly symmetric cell (cell 7608, layer 5 at 8.5°). (*A* and *D*) Isomodulation contour maps from SMT. (*B* and *E*) Polar plot of SAT position series. (*C* and *F*) SAT axis series. Same conventions as Fig. 2. For cell 6824, the center square evoked 67 spikes per s, the center circle evoked 98 spikes per s, and the full-screen evoked 115% inhibition, since the firing rate was suppressed below the rate of spontaneous activity. For cell 7608, these values were 105 and 104 spikes per s, and 85% inhibition. For cell 6824, the SI values were 0.19 (p1), 0.06 (p2), and 0.01 (a); for cell 7608 these values were 0.07, 0.12, and 0.03, respectively.

implementation in area MT based on directional derivatives of the flow (changes in flow velocity along a line in the image). Since surround influences generally possess the same speed and direction specificity as the CRF (refs. 10 and 18; D.-K.X. and G.A.O., unpublished results), an MT cell of the asymmetric type will be maximally driven when unequal velocities are presented over the CRF and the flanking inhibitory region, thus effectively taking the derivative of velocity along the line linking the two regions. Such a cell should be able to analyze slant in surfaces specified by motion, a possibility that appears likely in light of ongoing experiments (D.-K.X. and G.A.O., unpublished results). Similarly a bilaterally symmetric MT cell will be driven maximally when the velocity over the CRF differs from the speed over the two flanking regions and can be thought of as implementing a second-order directional derivative. This configuration would be responsive to surfaces curved in the direction parallel to the axis of the inhibition. Moreover, the second-order derivative indicates the direction of heading of ego motion, irrespective of the direction of derivation (25, 30). This could be achieved by bilaterally symmetric and by circularly symmetric surrounds (31).

Analysis via directional derivatives appears to be a recurring strategy throughout the primate visual system, starting with luminance in the case of simple cells (32, 33) and perhaps extending to texture or disparity gradients in the intermediate cortical visual areas cohierachical with area MT. The present demonstration that inhibitory regions outside the CRF of neurons in area MT also represent a local-to-local comparison mechanism may, therefore, have widespread implications for the entire primate visual system.

The technical assistance of P. Kayenbergh, G. Meulemans, and G. Vanparrijs is gratefully acknowledged. The comments of Drs. A. Sillito, H. Jones, R. Vogels, J. J. Vanderhaeghen, and O. Faugeras were invaluable in the preparation of this manuscript. We also express our gratitude to Janssens Pharmaceutica for their generosity in supplying the Sufentanil used in these experiments. This work was supported by grants from the Regional Ministry of Education (GOA 90/94-3) and the Commission of the European Communities (Esprit BRA Insight I and II).

1. Kuffler, S. W. (1953) *J. Neurophysiol.* **28,** 37–68.
2. McIlwain, J. T. (1964) *J. Neurophysiol.* **27,** 1154–1173.
3. Von Grunau, M. & Frost, B. J. (1983) *Exp. Brain Res.* **49,** 84–92.
4. Desimone, R., Schein, S. J., Moran, J. & Ungerleider, L. G. (1985) *Vision Res.* **25,** 441–452.
5. Zeki, S. M. (1983) *Neuroscience (New York)* **9,** 767–781.
6. Desimone, R. & Schein, S. J. (1987) *J. Neurophysiol.* **57,** 835–868.
7. Schein, S. J. & Desimone, R. (1990) *J. Neurosci.* **10,** 3370–3389.
8. Ghose, G. M., Roe, A. W. & Ts'o, D. Y. (1994) *Soc. Neurosci. Abstr.* **20,** 840.
9. Allman, J., Miezin, F. & McGuinness, E. (1985) *Perception* **14,** 105–126.
10. Lagae, L., Gulyas, B., Raiguel, S. & Orban, G. A. (1989) *Brain Res.* **496,** 361–367.
11. Born, R. & Tootell, R. (1992) *Nature (London)* **357,** 497–499.
12. Raiguel, S., Van Hulle, M., Marcar, V., Xiao, D.-K. & Orban, G. A. (1995) *Eur. J. Neurosci.*, in press.
13. Dubner, R. & Zeki, S. M. (1971) *Brain Res.* **35,** 528–532.
14. Maunsell, J. H. R. & Van Essen, D. C. (1983) *J. Neurophysiol.* **49,** 1127–1147.
15. Albright, T. D., Desimone, R. & Gross, C. G. (1984) *J. Neurophysiol.* **51,** 16–31.
16. Newsome, W. T. & Pare, E. B. (1988) *J. Neurosci.* **8,** 2201–2211.
17. Schiller, P. H. & Lee, K. (1994) *Visual Neurosci.* **11,** 229–241.
18. Tanaka, K., Hikosaka, K., Saito, H., Yukie, M., Fukada, Y. & Iwai, E. (1986) *J. Neurosci.* **6,** 134–144.
19. Tanaka, K., Sugita, Y., Madoka, M. & Saito, H.-A. (1993) *J. Neurophysiol.* **69,** 128–142.
20. Lagae, L., Maes, H., Raiguel, S., Xiao, D. & Orban, G. A. (1994) *J. Neurophysiol.* **71,** 1597–1626.
21. Allman, J., Miezin, F. & McGuinness, E. (1985) *Annu. Rev. Neurosci.* **8,** 407–430.
22. Albright, T. D. (1993) in *Visual Motion and Its Role in the Stabilization of Gaze*, eds. Miles, F. A. & Wallman, J. (Elsevier, Amsterdam), pp. 177–201.
23. Buracas, G. T. & Albright, T. D. (1994) *Adv. Neural Info. Process. Syst.* **6,** 966–976.
24. Nakayama, K. & Loomis, J. M. (1974) *Perception* **3,** 63–80.
25. Koenderink, J. & van Doorn, A. J. (1992) *J. Opt. Soc. Am.* **9,** 530–538.
26. Wohm, K. & Waxman, A. M. (1990) *Comput. Vision Graphics Image Process.* **49,** 127–151.
27. Anderson, R. A. & Siegel, R. (1986) *Soc. Neurosci. Abstr.* **12,** 1183.
28. Vogels, R. & Orban, G. A. (1994) *J. Neurophysiol.* **4,** 1428–1451.
29. Bishop, P. O., Coombs, J. S. & Henry, G. H. (1971) *J. Physiol. (London)* **219,** 659–687.
30. Koenderink, J. & van Doorn, A. J. (1991) *J. Opt. Soc. Am.* **8,** 377–385.
31. Carmen, G. J. (1991) *Soc. Neurosci. Abstr.* **17,** 847.
32. Jones, J. P. & Palmer, L. A. (1978) *J. Neurophysiol.* **58,** 1233–1258.
33. Daugman, J. G. (1985) *J. Opt. Soc. Am.* **2,** 1160–1169.